# Detection of Superoxide Ions from Photoexcited Semiconductors in Non-Aqueous Solvents Using the ESR Spin-Trapping Technique

Hiroyuki NODA,* Kazuo OIKAWA,† Hiroaki OHYA-NISHIGUCHI, and Hitoshi KAMADA
Institute for Life Support Technology, Yamagata Technopolis Foundation, 683 Kurumanomae, Numagi, Yamagata 990
† Yamagata Research Institute of Technology, 683 Kurumanomae, Numagi, Yamagata 990
(Received March 18, 1993)

The ESR spin-trapping technique using 5,5-dimethyl-1-pyrroline *N*-oxide (DMPO) and *N*-*t*-butylbenzylideneamine *N*-oxide (PBN) as spin-trap reagents has been applied to detect active oxygen radicals generated by the photoexcitation of powdery semiconductors ($TiO_2$, $WO_3$, CdS, and $Fe_2O_3$) in non-aqueous solvents such as dimethylsulfoxide (DMSO), benzene, ethanol, and acetonitrile. Appreciable amounts of superoxide ion ($O_2^-$) were detected from $TiO_2$, $WO_3$, $Fe_2O_3$, and CdS suspensions under photoexcitation. The hyperfine splitting constants (hfsc) of the superoxide ion and carbon(C)-centered radical spin adducts for DMPO and PBN could be determined in various non-aqueous solvents. Some characteristic features for the production of the superoxide ion and C-centered radicals are discussed in connection with the energy-level diagrams of the semiconductors and the redox potentials of the superoxide ion and non-aqueous solvents.

In our previous studies[1,2] the detection of active oxygen radicals, such as the superoxide ion ($O_2^-$), hydroperoxyl radical ($\cdot O_2H$), and hydroxyl radical ($\cdot OH$) produced from photoexcited semiconductors ($TiO_2$, $WO_3$, CdS, and $Fe_2O_3$) in water and aqueous $H_2O_2$ solutions, was performed by the use of an ESR spin-trapping technique. It was found that the superoxide ion is produced from the reduction of dissolved oxygen by a photoproduced electron, the hydroperoxyl radical is generated from the oxidation of $H_2O_2$ by a photoproduced hole, and the hydroxyl radical is produced from the oxidation of water by a photoproduced hole and from the reduction of $H_2O_2$ by a photoproduced electron. Moreover, the mechanism for the generation of active oxygen radicals from photoexcited semiconductors in aqueous media could be rationalized in terms of the valence band and conduction band edges of the semiconductors, the redox potentials of the active oxygen radicals, and the surface acidity and basicity of the semiconductors.

When semiconductors are used as a cancer-killing agent,[3] the reactions between the active oxygen radicals and the cancer cell must occur in both aqueous and non-aqueous media, since powdery semiconductors are distributed on the cell membrane and in the cytoplasm.[3] It is thus important that the behavior of the active oxygen radicals from photoexcited semiconductors are examined in both media. Moreover, the reactions between the photogenerated holes and the organic compounds in the cell membrane etc. are also important, because those of the cell membrane with low oxidation potentials are easily attacked by photogenerated holes.

A few papers[4,5] have been published concerning the production of active oxygen radicals from photoexcited semiconductors in non-aqueous media, compared with those in aqueous media.[1,2,6—10] For example, Harbour and Hair[4] reported the production of the superoxide ion from photoexcited CdS in non-aqueous media, in addition to that in aqueous media using 5,5-dimethyl-1-pyrroline *N*-oxide (DMPO) as a spin-trap reagent. The detected superoxide ion was explained to be produced from a reduction of dissolved oxygen by photogenerated electrons. Moreover, they pointed out that the superoxide ion or hydroperoxyl radical played a crucial role as the reaction intermediate for the photooxidation of various alcohols.[11] However, the mechanisms for the generation of active oxygen radicals from photoexcited semiconductors in non-aqueous media have not been very clearly elucidated.

In order to examine the mechanism for the generation of superoxide ion in non-aqueous media we carried out systematical experiments involving the spin trapping of intermediates produced during irradiation of powdery semiconductors in several non-aqueous solvents. In this paper we describe a possible mechanism for the reaction of photoexcited semiconductors using dissolved oxygen and non-aqueous solvents.

## Experimental

**Materials.** Powdery semiconductors [$TiO_2$ (99.9%, rutile and anatase), CdS (practical grade), $WO_3$ (99.5%), and $Fe_2O_3$ (99.9%)] were purchased from Wako Pure Chemical Industries, Ltd. 5,5-Dimethyl-1-pyrroline *N*-oxide (DMPO) was obtained from Dojindo Laboratory. *N*-*t*-butylbenzylideneamine *N*-oxide (PBN) and potassium superoxide ($KO_2$) were obtained from Aldrich Chem., Co. Non-aqueous solvents (special grade) from Kanto Chemical Co., Inc. were used without further purification.

**ESR Measurements.** A flat, quartz ESR cell was used in all of the experiments. A powdery semiconductor (1—5 mg) was mixed with 90 μl of non-aqueous solvent and 10 μl of 9.2 mol dm$^{-3}$ DMPO (or 1 mol dm$^{-3}$ PBN) in respective non-aqueous solvents. The suspension was then fed into the ESR cell, which was inserted into the cavity of an ESR spectrometer (JEOL JES-RE2X). The sample was irradiated with a 500-W xenon lamp for 30-120 s. A 370-nm or 420-nm interference filter was used for illuminating $TiO_2$ and $WO_3$, or other semiconductors, thus causing band-gap excitation, but excluding the effect of short-wavelength

ultraviolet light. ESR measurements were conducted under the following conditions: magnetic field, 336±5 mT; field modulation, 0.1 or 0.125 mT; time constant 0.03 or 0.1 s; microwave power, 8 mW; sweep time, 5 mT min$^{-1}$.

## Results

**Reactions in DMSO.** When the semiconductor suspensions described in experimental section were irradiated with an energy greater than the band-gap energy (anatase, 3.2 eV; rutile, 3.0 eV; $WO_3$, 2.8 eV; CdS, 2.4 eV; and $Fe_2O_3$, 2.2 eV) in DMSO, the ESR spectra of the DMPO spin adducts were observed, as shown in Fig. 1. The spectra of Fig. 1a to c (anatase, rutile, and $WO_3$) mainly comprise two signals: One is easily identified as being the superoxide ion spin adduct in view of hyperfine splitting constant (hfsc) values of $a_N=1.28$ mT, $a_H^{\beta}=1.05$ mT, and $a_H^{\gamma}=0.14$ mT;[3] the other is identified as being the methyl radical spin adduct with hfsc values of $a_N=1.50$ mT and $a_H^{\beta}=2.11$ mT, which was produced by the oxidation of DMSO. Another spin adduct with hfsc values of $a_N=1.38$ mT and $a_H^{\beta}=1.14$ mT is also shown in Fig. 1a—c. This spin adduct is expected to be a sulfur(S)-centered spin adduct, since it was observed in conjunction with the methyl radical spin adduct when DMSO was used as a solvent, and was not observed in the cases of the other non-aqueous solvents (as shown in Figs. 2, 3, and 4). We thus assigned it to an S-centered radical.

The hfsc values of the superoxide ion spin adducts obtained in the systems of anatase, rutile, and $WO_3$ were in line with those obtained from $KO_2$ contained in DMSO ($K^+ + O_2^-$). It is noted here that the intensity for $WO_3$ was smaller than those for $TiO_2$ and CdS. Under a deaerated condition this signal intensity decreased appreciably. The spectrum of Fig. 1d (CdS) also comprises a signal from the superoxide ion spin adduct in view of the same hfsc values as those from former three semiconductors. This result is in line with the result of Harbour and Hair.[4] The spectrum of Fig. 1e ($Fe_2O_3$) comprises trace amounts of the signals from the S-centered spin adduct and from that of the superoxide ion spin adduct.

**Reactions in Other Solvents.** The mechanism for the generation of the superoxide ion was expected to be clarified by experiments with various non-aqueous solvents. The ESR spectra from the semiconductors in benzene, ethanol, and acetonitrile are shown in

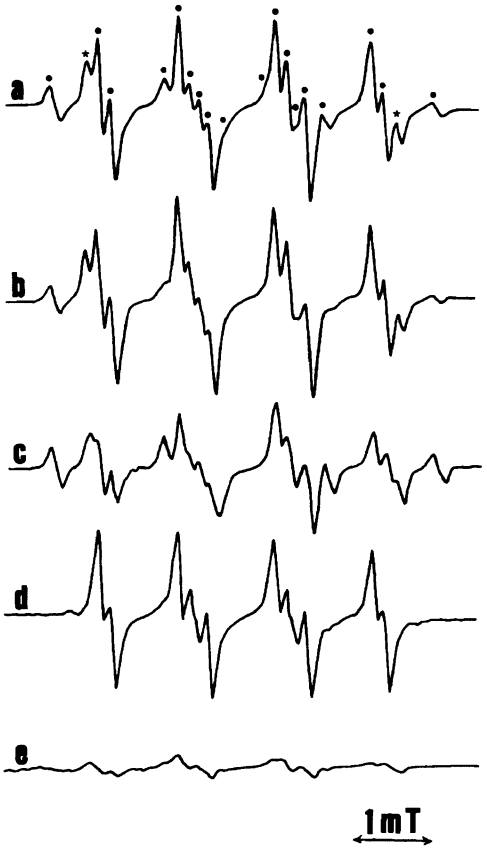


Fig. 1. ESR spectra of the DMPO spin adducts obtained by photoexcitation of semiconductors in DMSO. a: anatase $TiO_2$, b: rutile $TiO_2$, c: $WO_3$, d: CdS, e: $Fe_2O_3$, irradiation wavelength: 370 nm (a—c), 420 nm (c, d), receiver gain: ×100 (a and b), ×200 (others), open circle: DMPO–OOH, closed circle: DMPO–centered, star: unknown spin adducts.

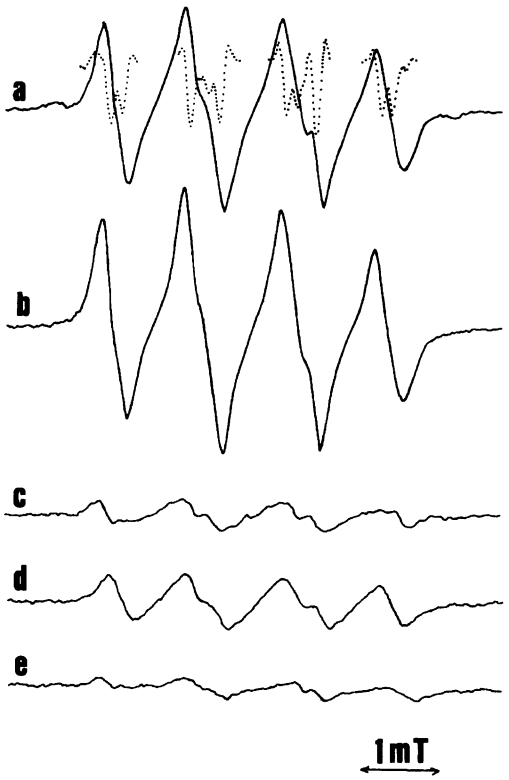


Fig. 2. ESR spectra of the DMPO spin adducts obtained by photoexcited semiconductors in benzene. a: anatase $TiO_2$ and the dotted line is the second harmonic mode, b: rutile $TiO_2$, c: $WO_3$, d: CdS, e: $Fe_2O_3$, irradiation wavelength: same as Fig. 1, receiver gain: ×200.

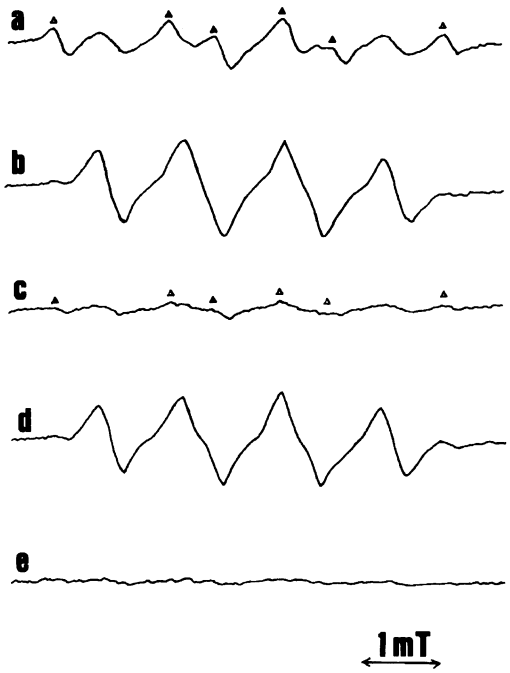


Fig. 3. ESR spectra of the DMPO spin adducts obtained by photoexcited semiconductors in ethanol. a: anatase $TiO_2$, b: rutile $TiO_2$, c: $WO_3$, d: CdS, e: $Fe_2O_3$, irradiation wavelength: same as Fig. 1, receiver gain: ×200, open triangle: DMPO-centered.

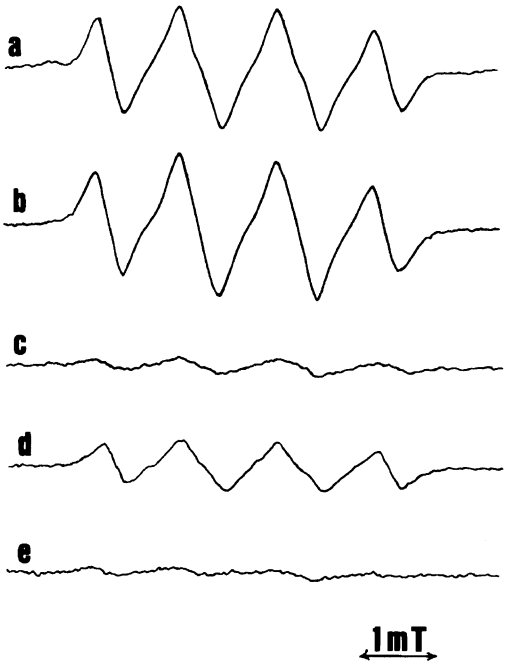


Fig. 4. ESR spectra of the DMPO spin adducts obtained by photoexcited semiconductors in acetonitrile. a: anatase $TiO_2$, b: rutile $TiO_2$, c: $WO_3$, d: CdS, e: $Fe_2O_3$, irradiation wavelength: same as Fig. 1, receiver gain: ×200.

Fig. 2 to Fig. 4. In these media broad ESR spectra were observed from the photoexcitation. These broadenings were caused by a high concentration of dissolved oxygen,[3] because the solubility of oxygen in these solvents were in the order DMSO<benzene≈ethanol≈acetonitrile.[12,13] These signals were all assigned to the superoxide ion spin adducts based on ESR measurements of the second-harmonic mode, as shown by the dotted line of Fig. 2a. The hfsc values of the superoxide ion spin adduct observed in benzene were determined to be $a_N=1.26$ mT, $a_H^{\beta}=1.04$ mT, and $a_H^{\gamma}=1.5$ mT, which are consistent with the results of Mitsuta et al.[14] The intensities of the spin adduct obtained from the semiconductors in benzene showed a trend that is similar to those obtained in DMSO. However, the DMPO spin adduct of the phenyl radical was not clearly observed. This may have arisen from the low trapping efficiency of DMPO for the phenyl radical. Therefore, the production of the phenyl radical was confirmed by the use of PBN as another trapping reagent. The results are described later.

In Figs. 3 and 4, similar trends concerning the spectral patterns of the spin adduct were observed in ethanol and acetonitrile, except for the cases of anatase $TiO_2$ and $WO_3$ in ethanol. The observed spin adduct from rutile $TiO_2$ and CdS showed the same hfsc values of $a_N=13.3$ mT (ethanol), 13.1 mT (acetonitrile) and $a_H^{\beta}=10.3$ mT (ethanol, acetonitrile). Unfortunately, the value of $a_H^{\gamma}$ was not determined in these solvents. This may also have arisen from dissolved oxygen. These adducts can also be assigned to the superoxide ion spin adduct.[14] The intensities of the spin adduct observed in ethanol and acetonitrile were smaller than those observed in DMSO and benzene. These are believed to be related to the probability for the separation of a photogenerated electron-hole pair, depending on the difference in the oxidation potentials of non-aqueous solvents.

In ethanol, a spin adduct having hfsc values of $a_N=$ 14.9 mT and $a_H^{\beta}=21.4$ mT was observed from anatase $TiO_2$ and $WO_3$ in addition to the superoxide ion spin adduct under aerated conditions. This adduct can be assigned to the C-centered spin adduct [$\cdot CH(CH_3)OH$], as Yamagata et al. reported previously.[11] Under the deaerated condition, only the C-centered adduct was observed from rutile and anatase $TiO_2$. This fact, therefore, indicates that the photocatalytic reactions under aerated conditions are different from those under deaerated conditions. The spectral difference between anatase (Fig. 3a) and rutile (Fig. 3b) may have arisen from the difference in the adsorption of oxygen and ethanol, which is caused by difference in their surface acidity ($WO_3$>anatase>rutile).[2] A small intensity of the ESR signals was observed from photoexcited $Fe_2O_3$ in ethanol and acetonitrile.

The hfsc values of the DMPO spin adducts obtained from photoexcited semiconductors are summarized in Table 1.

**Spin Trapping by PBN.** A comparison of the data, which were obtained from experiments using two

Table 1. The hfsc Values of the DMPO Spin Adducts Obtained in This Study

| Solvent | DMPO–OOH | | | DMPO–C–centered | |
|---|---|---|---|---|---|
| | $a_N$ | $a_H^\beta$ | $a_H^\gamma$/mT | $a_N$ | $a_H^\beta$/mT |
| DMSO | 1.29 | 1.04 | 0.14[a] | 1.50 | 2.11[e] |
| Benzene | 1.26 | 1.04 | 0.15[b] | | |
| Ethanol | 1.33 | 1.03[c] | | 1.49 | 2.14[f] |
| Acetonitrile | 1.31 | 1.03[d] | | | |

a) From anatase, rutile, $WO_3$, and CdS. b) From anatase, rutile, $WO_3$, and CdS. c) From anatase, rutile, and CdS. d) From anatase, rutile, and CdS. e) $\cdot CH_3$, from anatase, rutile, and $WO_3$. f) $\cdot CH(CH_3)OH$, from anatase.

or more spin-trap reagents, is profitable for assigning the produced intermediates. In our study, PBN was used as another spin-trap reagent. The ESR spectra of PBN spin adducts from anatase $TiO_2$ in various non-aqueous solvents are shown in Fig. 5. The spectrum of Fig. 5a comprises a signal from the C-centered (methyl) radical spin adduct in view of the hfsc values of $a_N=1.40$ mT and $a_H^\beta=0.23$ mT.[15] The intensity of the spin adduct was stronger than those of the DMPO spin adducts shown in Fig. 1. Therefore, the PBN is more sensitive than DMPO in trapping the C-centered radical. The spectrum of Fig. 5b comprises a signal from the phenyl radical spin adduct in view of the hfsc values of $a_N=1.39$ mT and $a_H^\beta=0.21$ mT.[15] Production of the phenyl radical, which was not confirmed by experiments using DMPO, was confirmed by using PBN. The spectrum in Fig. 5c comprises a spin adduct with hfsc values of $a_N=1.44$ mT and $a_H^\beta=0.32$ mT, which can be assigned to the C-centered radical [$\cdot CH(CH_3)$-OH] based on the results of experiments using DMPO. The spectrum of Fig. 5d can be assigned to the superoxide ion spin adduct ($a_N=1.40$ mT and $a_H^\beta=0.25$ mT) based on the results of experiments using DMPO. The hfsc values of PBN spin adducts observed from rutile $TiO_2$ and $WO_3$ are listed in Table 2 along with the hfsc values from anatase $TiO_2$. Thus, the results observed from experiments using PBN nicely support those obtained from experiments using DMPO. The increase in the polarity of the solvents led to an increase in the hfsc values of $a_N$ for DMPO and PBN spin adducts of the superoxide ion (solvent effect). The polarity of the solvents are in the order ethanol>acetonitrile>DMSO>benzene.[3] A few of the hfsc values of the superoxide ion spin adduct for PBN were observed in non-aqueous solvents.[15] Therefore, the hfsc values of the superoxide ion spin adduct for PBN observed in this study (Table 2) are useful for assigning the superoxide ion in non-aqueous media.

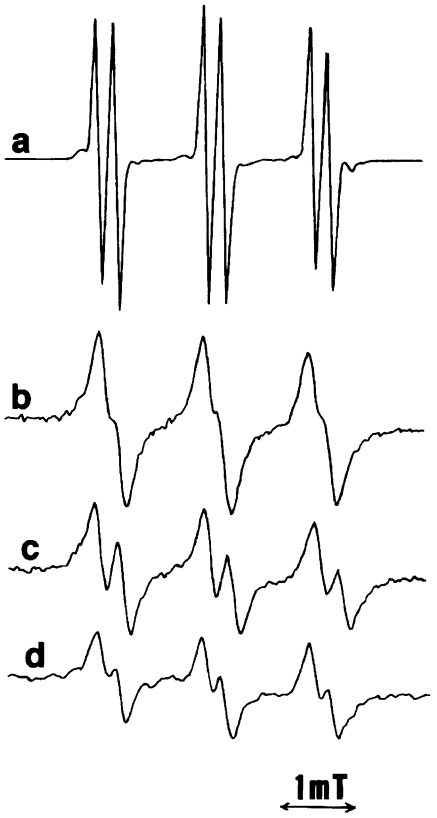


Fig. 5. ESR spectra of the PBN spin adducts obtained by photoexcited anatase $TiO_2$ in four non-aqueous solvents. a: DMSO, b: benzene, c: ethanol, d: acetonitrile.

## Discussion

It is well established that the oxidation potentials (half-wave potential, $E_{1/2}$) of organic compounds linearly correlate with their photoionization potentials (IP). In Fig. 6, $E_{1/2}$ of several organic compounds in acetonitrile are plotted against their IP.[16—19] Using this relationship, the oxidation potentials of DMSO (IP=9.11 eV) and acetonitrile (IP=12.12 eV) can be estimated to be 2.4 and 4.0 V vs. NHE, respectively. The energy band structures of the semiconductors and the redox potentials of the superoxide ion and those of non-aqueous solvents thus estimated are schematically depicted in Fig. 7.[20,21]

The superoxide ion adduct was produced from all of the semiconductors used. Such a production of the su-

Table 2. The hfsc Values of PBN Spin Adduct Obtained in This Study

| Solvent | PBN–OOH | | PBN–C–centered | |
|---|---|---|---|---|
| | $a_N$ | $a_H^\beta$/mT | $a_N$ | $a_H^\beta$/mT |
| DMSO | 1.38 | 0.15[a] | 1.40 | 0.23[e] |
| Benzene | 1.35 | 0.17[b] | 1.39 | 0.21[f] |
| Ethanol | 1.42 | 0.22[c] | 1.44 | 0.32[g] |
| Acetonitrile | 1.40 | 0.25[d] | | |

a) From rutile and CdS. b) From rutile and CdS. c) From rutile and CdS. d) From anatase, rutile, and CdS. e) $\cdot CH_3$, from anatase and rutile. f) $\cdot C_6H_5$, from anatase and rutile. g) $\cdot CH(CH_3)OH$, from anatase.

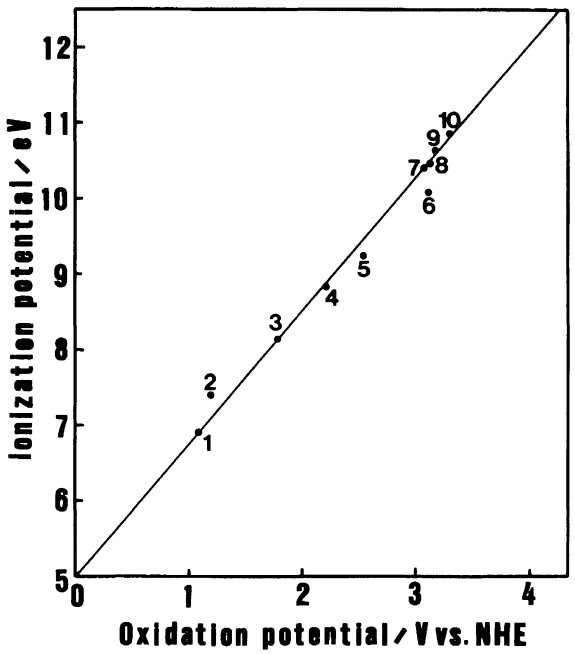


Fig. 6. Plot of photoionization potentials against oxidation potentials of organic compounds. 1: perylene, 2: anthracene, 3: naphthalene, 4: toluene, 5: benzene, 6: 2-butanol, 7: 2-propanol, 8: 1-propanol, 9: ethanol, 10: methanol.

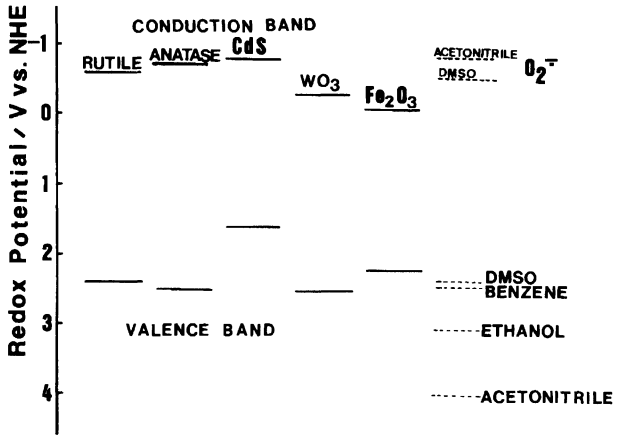


Fig. 7. Energy band structures of semiconductors and the redox potentials of superoxide ion and non-aqueous solvents.

peroxide ion is believed to originate in photoproduced electrons. However, the mechanism for the production of the superoxide ion in non-aqueous solvents cannot always be explained by using the scheme of Fig. 7. This is because the reactivity of the semiconductors is also influenced by the particle size, the mobility of the electron and hole, an effect of the electrical potential floating,[22] and the adsorption behavior of oxygen and solvent molecules to the semiconductor surface.

The following trends, however, can be found in an analysis of these results: The superoxide ion adduct is easily produced from semiconductors, such as anatase and rutile $TiO_2$ and CdS, in that the conduction-band edges locate above the oxygen reduction potential, as shown in Fig. 7. Furthermore, the superoxide ion adduct is also produced from photoexcited semiconductors, such as $WO_3$ and $Fe_2O_3$, in which the conduction-band edges are located below the oxygen reduction potential, even though their intensities are appreciably small. This result may have arisen from a negative shift of the particle charge due to an effect of the electrical potential floating in non-aqueous media or an energy-level spreading due to a distribution of the oxygen reduction potential. Therefore, one should understand the intensity change as being a result of all the effects described above.

The production of the superoxide ion and C-centered adducts from anatase and rutile $TiO_2$ and $WO_3$ are also influenced by the oxidation potentials of non-aqueous solvents. In fact, the observed intensities of the superoxide ion adducts in DMSO and benzene are larger than those in ethanol and acetonitrile having high oxidation potentials in which their highest occupied levels lie below the valence-band edges of the semiconductors. On the other hand, the C-centered adducts are produced from photoexcited semiconductors, such as anatase and rutile $TiO_2$ and $WO_3$, in which their valence-band edges are located below (or near) to the oxidation potentials of non-aqueous solvents. This correspondence in any case indicates that the generated holes in the semiconductors oxidize the solvent molecules on their surface, which are converted into C-centered radicals. In ethanol and acetonitrile systems without any production of the C-centered radical, however, the photoproduced holes are accumulated and recombine with photoproduced electrons in semiconductors. This recombination results in a low efficiency of the superoxide ion production in these solvents, as described above.

In conclusion, it has been demonstrated by using the ESR spin-trapping technique that the superoxide ion is produced from photoexcited semiconductors (anatase, rutile, $WO_3$, $Fe_2O_3$, and CdS) and the C-centered radicals are produced from $TiO_2$ and $WO_3$ in non-aqueous solvents. Some trends for their production from photoexcited semiconductors in non-aqueous media have been rationalized in terms of the energy-level diagrams of the semiconductors and the redox potentials of the superoxide ion and non-aqueous solvents. The hfsc values of DMPO and PBN spin adducts for the superoxide ion and C-centered radical in various non-aqueous solvents could be determined by using of the photoexcited semiconductors. Photoexcited semiconductor systems will be useful for determining the hfsc values of the spin-trap reagents.

This study was performed through Special Coordination Funds of the Science and Technology Agency and the Yamagata Technopolis Foundation.

## References

1) H. Noda, K. Oikawa, and H. Kamada, *Bull. Chem. Soc. Jpn.*, **65**, 2505 (1992).
2) H. Noda, K. Oikawa, and H. Kamada, *Bull. Chem. Soc. Jpn.*, **66**, 455 (1993).
3) R. Cai, K. Hashimoto, K. Itoh, Y. Kubota, and A. Fujishima, *Bull. Chem. Soc. Jpn.*, **64**, 1268 (1991).
4) J. R. Harbour and M. L. Hair, *J. Phys. Chem.*, **82**, 1397 (1978).
5) C. Chen, R. P. Veregin, J. R. Harbour, M. L. Hair, S. L. Issler, and J. Tromp, *J. Phys. Chem.*, **93**, 2607 (1989).
6) J. R. Harbour and M. L. Hair, *J. Phys. Chem.*, **81**, 1791 (1977).
7) C. D. Jaeger and A. J. Bard, *J. Phys. Chem.*, **83**, 3146 (1979).
8) E. M. Cresa, L. Burlamacchi, and M. Visca, *J. Mater. Sci.*, **18**, 289 (1983).
9) J. R. Harbour and M. L. Hair, *Adv. Colloid Interface Sci.*, **24**, 103 (1986).
10) A. Maldotti, R. Amadelli, and V. Carassiti, *Can. J. Chem.*, **66**, 76 (1988).
11) S. Yamagata, S. Nakabayashi, K. M. Sancier, and A. Fujishima, *Bull. Chem. Soc. Jpn.*, **61**, 3429 (1988).
12) R. A. Greenwald, "Handbook of Method for Oxygen Radical Research," CRC Press, Florida (1985), p. 65.
13) H. Stephen and T. Stephen, "Solubilities of Inorganic and Organic Compounds," Pergamon Press, Oxford (1963).
14) K. Mitsuta, M. Kohno, Y. Mizuta, M. Yamada, and M. Aoyama, *Zikikyomei to Igaku*, **2**, 190 (1991).
15) G. R. Buettner, *Free Radical Biol. Med.*, **3**, 259 (1987).
16) K. S. Pysh and N. C. Yang, *J. Am. Chem. Soc.*, **85**, 2124 (1963).
17) G. Sundholm, *Acta Chem. Scand.*, **25**, 3188 (1971).
18) J. W. Robinson, "Handbook of Spectroscopy," CRC Press, Florida (1974), p. 257.
19) K. Kimura, S. Katsumata, Y. Achiba, T. Yamazaki, and S. Iwata, "Handbook of HeI Photoelectron Spectra of Foundamental Organic Molecules," Japan Scientific Societies Press, Tokyo (1981).
20) Nippon Kagaku kai, "Kagaku Sosetsu No. 39, Muki Kokagaku," Gakkai Shuppan Center, Tokyo (1983), p. 118.
21) Nippon Kagaku Kai, "Kikan Kagaku Sosetsu No. 7, Kassei Sanso No Kagaku," Gakkai Shuppan Center, Tokyo (1990), p. 3.
22) Y. Aikawa, A. Takahashi, and M. Sukigara, *Nippon Kagaku Kaishi*, **1984**, 292.